



Investigation on Tribological Behavior of Hot-Pressed Steel/TiB₂ Composites Using Taguchi Experimental Design

Silani Sahoo, Bharat Bhusan Jha, Sisir Mantry, Sandip Kumar Nayak , Tarasankar Mahata, Jyothi Sharma, Tammana SRCh Murthy, and Animesh Mandal

Submitted: 4 June 2021 / Revised: 22 September 2021 / Accepted: 8 October 2021 / Published online: 29 October 2021

This article presents the dry sliding wear response of steel composites reinforced with TiB₂ particles prepared by hot consolidation. Taguchi's L₂₇ orthogonal array design is adopted to investigate the effect of four operating parameters, i.e., normal load, sliding speed, sliding distance, and reinforcement content on the wear rate of the resultant composite. Reinforcement content is observed to be the most significant factor that affects the wear mechanism followed by sliding velocity and normal load. Specific wear rate revealed a decreasing trend with an increase in sliding speed and load. Wear mechanisms were discussed by analyzing the worn surfaces using a scanning electron microscope. The presence of hard TiB₂ particles resulted in enhancement of resistance to plastic deformation of the steel matrix by preventing plastic plowing and cutting.

Keywords ANOVA, hot pressing, sliding wear, steel composite, Taguchi experimental design

1. Introduction

Metal matrix composites (MMCs) provide superior combinations of desirable properties such as high thermal stability, strength, stiffness, wear, and corrosion resistance, essential for many applications. MMCs are superior to alloying additions or precipitation hardened steels due to the second phase thermal stability. Hence, MMCs are the center of research and development attention in automotive, aerospace, and other associated sectors. Composites can adopt different situations with judicious combinations of matrix and reinforcement materials to exhibit desired properties for specific applications (Ref 1, 2). The utilization of iron-based alloy or steels as the matrix materials for MMCs has recently fascinated extensive

consideration due to its low cost, adaptability, and desirable mechanical properties (Ref 3-5). In this context, Qiu et al. (Ref 6) reported significant improvement in the strength and toughness of cast medium carbon steel by the reinforcement of nano-sized TiC particles. However, tribological application of austenitic stainless steels is limited owing to its low hardness and wear performance. Incorporation of ceramic particulates like oxides, carbides, borides into steel matrices is an effective means for enhancement of mechanical and tribological applications (Ref 7, 8). In general, the reinforcement material used in composite production plays a vital role in improving the strength, creep strength, and wear performance of the material. The influence of the addition of particles on the tribological performance of composites is a complicated matter. Therefore, the investigation of wear behavior of steel-based materials is becoming increasingly important (Ref 9, 10). Several researchers have explored the wear performance of steel composite reinforced with hard particles. For example, Akhtar et al. (Ref 11) employed powder metallurgy route to produce steel composite reinforced with 50 wt.% to 70 wt.% TiC. The authors investigated the fretting wear behavior of the developed composite against high-speed steel. They reported micro ploughing of the stainless steel as a dominant wear mechanism and severe wear at higher wear loads and low content of TiC. Pagounis et al. (Ref 12) reported increased wear resistance of the steel by adding ceramic reinforcement particles.

Mechanical and tribological performance of spark plasma sintered 316L stainless steel composites with TiB₂ sub-micro particles were investigated by Sulima and her group (Ref 13). The results showed a significant influence of sintering parameters and TiB₂ content on tribological behavior of the composite. Tjong et al. (Ref 14) reported that the addition of TiB₂ particles is very useful in improving the wear resistance of soft and ductile austenitic stainless steel. In their subsequent work (Ref 15), they studied the two-body abrasive wear behavior of stainless composites reinforced with various volume fractions of TiB₂ particles. They reported that TiB₂

Silani Sahoo, Advanced Materials Technology Department, CSIR-Institute of Minerals and Materials Technology, Bhubaneswar, Odisha 751013, India; **Bharat Bhusan Jha**, Metallurgy and Materials Engineering, National Institute of Technology, Jamshedpur, Jharkhand 831014, India; **Sisir Mantry**, Materials Chemistry Department, CSIR-Institute of Minerals and Materials Technology, Bhubaneswar, Odisha 751013, India; **Sandip Kumar Nayak**, Mechanical Engineering Department, National Institute of Technology, Rourkela, Odisha 769008, India; **Tarasankar Mahata** and **Jyothi Sharma**, Powder Metallurgy Division, Bhabha Atomic Research Centre, Navi Mumbai, Maharashtra 400703, India; **Tammana SRCh Murthy**, Materials Processing and Corrosion Engineering Division, Bhabha Atomic Research Centre, Mumbai, Maharashtra 400 085, India; **Animesh Mandal**, School of Minerals, Metallurgical and Materials Engineering, Indian Institute of Technology Bhubaneswar, Bhubaneswar, Odisha 751007, India. Contact e-mail: nayak.sandip200@gmail.com.

particles are effective enough to reduce cutting efficiency of abrasive particles, thereby enhancing wear performance. Song and his co-workers (Ref 16) investigated the wear performance of ferrous matrix composites with WC_p reinforcement at 400 °C. They concluded a marked increase in wear rate with applied load and testing temperature. Degnan et al. (Ref 17) produced TiC reinforced steel composite by liquid-phase process approach by using self-propagating high temperature synthesized additive powder. They observed improved wear resistance over its unreinforced counterpart under low levels of loading varying from 90 N-360 N and at room temperature. In an identical investigation, Deng et al. (Ref 18) investigated the three-body abrasion wear resistance of low-alloy martensitic steel reinforced with TiC under dry and wet sliding condition. They reported that the resistance to three-body abrasion of steel is increased with the reinforcement of TiC particles. However, the resistance to wear in dry condition was superior to the resistance to wear in wet condition.

Although many researchers have studied the wear behavior of steel composites, investigation on the selection of optimal wear parameters still lacks in the literature. The prevailing literature reported the influence of composites wear performance by various factors such as sliding distance, normal load, sliding speed, reinforcement content, shape, and size. So, it is essential to know the effects of different factors and their interaction on wear behavior of steel composites. Many researchers have utilized several statistical models such as the design of experiments (DOE), factorial design model, artificial neural network, factorial design model, Taguchi's design approximation, genetic algorithm, and response surface model to understand the interaction between input variables on the output (Ref 19, 20). Taguchi technique is the most widely used DOE tool in industries as it is a systematic approach, efficient and straightforward to optimize designs for quality, cost, and performance (Ref 21-23). Dharmalingam et al. (Ref 24) adopted the Gray-Taguchi method to optimize aluminum metal matrix composite's dry sliding performance. They concluded that testing parameters have a significant influence on the wear properties. Baskaran et al. (Ref 25) examined the effect of different controlling factors on dry sliding wear response of in-situ cast AA7075-TiC composites by employing Taguchi L₂₇ orthogonal array experimental design. They discussed significant contributing parameters on the wear rate using ANOVA analysis and reported the optimum parameter combination by conducting the confirmation test. Girish et al. (Ref 26) conducted the wear performance of magnesium alloy (AZ91) hybrid metal matrix composites using the Taguchi technique. They estimated the effect of parameters on wear rate by using the signal-to-noise ratio and analysis of variance. They developed a linear regression equation using MINITAB 17 program and observed good agreement between predicted and actual wear rate. Koksai et al. (Ref 27) also adopted Taguchi's method to develop a wear rate prediction model for aluminum-based composites reinforced with aluminum diboride (AlB₂) flakes. Authors have observed applied load as the influential critical parameter with a contribution of 58.2% on the specific wear rate followed by reinforcement content and sliding velocity.

Based on existing literature, it is evident that the researchers have performed no work to examine the impact of testing parameters on the wear rate of steel composites using the Taguchi design of experiments. Therefore, an attempt is made to study the influence of reinforcement content, applied load,

sliding speed, and sliding distance on the wear behavior of the hot-pressed TiB₂ particle reinforced steel composites by adopting the Taguchi design of experiments. It is expected that the presented work outcomes will help in the optimization of process parameters effectively and will ensure the reliability of steel-based composites with desired properties for different applications.

2. Materials and Methods

TiB₂ particle reinforced steel composite was fabricated by the powder metallurgy process in the present work. Firstly, homogenous mixing of AISI 304 stainless steel powder with average particle size 28 μm (distribution range 20-35 μm) was performed with weighed quantity (2 vol.% and 4 vol.%) of TiB₂ reinforced particles having average size 2 μm (distribution range 1.4-2.6 μm). The mixing of powder was performed by using a planetary ball mill (Retsch, PM -400, Germany) with a ball to powder ratio (BPR) 10:1 at 200 rpm for 2 h in order to obtain homogeneous mixture (Ref 28). Milling was carried out then hot consolidation was conducted by employing a uniaxial vacuum hot pressing system (Vacuum Tech. Pvt. Ltd., India) at a temperature of 1100 °C for 15 minutes under 48 MPa. The heating rate was maintained at about 25 °C/min (Ref 29) (Ref 30, 31). Finally, a coin-shaped disc having a diameter of 30 mm was obtained. Detailed descriptions of the fabrication method and microstructure of the composite are found elsewhere (Ref 28). Dry sliding wear tests were conducted according to ASTM standard G99 using a pin-on-disc tribometer (DUCOM TR-20LE, India). In this test, high chromium 100Cr₆ ball of diameter 5mm was used as the pin specimens. Before testing, the samples were polished up to 1 μm finish and cleaned with acetone. Testing was executed at three different sliding velocities of 0.08 m/s, 0.11 m/s, and 0.13 m/s over sliding distances of 141 m, 188 m, and 235 m. Normal loads of 25 N, 30 N and 35 N were employed during the test. The test trials for each parameter combinations are repeated for three times and the average values are considered as the wear loss. The underlying wear mechanism was studied by analysis of worn surfaces using scanning electron microscopy. The depth of wear was measured automatically with a linear varied differential transducer (LVDT) and a data acquisition system provided with the tribometer. The wear volume and specific wear rate was calculated as

$$\text{Wear volume (mm}^3\text{)} = \frac{\text{Massloss(g)}}{\text{Density}(\frac{\text{g}}{\text{mm}^3})} \quad \text{and}$$

$$\text{Specific wear rate (m}^3\text{/N.m)} = \frac{\text{Wear volume(m}^3\text{)}}{\text{Sliding distance(m)} \times \text{Load(N)}}$$

respectively (Ref 32).

2.1 Experimental Design

Statistical methods are generally adopted to test a product's quality by minimizing the effort and time (Ref 33). These methods are useful for the investigation of the influence of different parameters on the product. The impact of control factors on performance output can be effectively investigated by the design of experiments (DOE). The most vital step in the design of the experiment is the selection of appropriate control factors. Non-significant variables are recognized at the earliest by considering a large number of factors initially. Taguchi method is an economical design method used to decide the most appropriate and streamlined control factor combinations,

with the minimum number of investigations (Ref 34, 35). In the sliding wear process, the wear rate is influenced by many input factors. The four crucial control factors, namely sliding velocity, reinforcement content, normal load, and sliding distance, were selected in the present work. $L_{27} (3^3)$ orthogonal array design was adopted in order to study the effect of selected control factors on the sliding wear performance of hot-pressed samples. Table 1 shows the selected control factors and their levels.

Table 2 presents the sliding wear trials and their performance output as per L_{27} orthogonal design. Signal-to-noise ratios (S/N) were estimated from the output results, as shown in Table 2. In the current work, the S/N ratio was calculated under “smaller is better” characteristics due to consideration of minimum wear rate, which is expressed as $\frac{S}{N} = -10 \log_{10} \frac{1}{n} (\sum y^2)$ with ‘n’ as the number of observations and ‘y’ as the observed data (Ref 36). Furthermore, the contribution ratio of each control factor was estimated by analysis of variance (ANOVA). ANOVA is a statistical technique that uses

Table 1 Control factors with their selected levels

Control factor	Levels			Units
	I	II	III	
A: Sliding velocity	0.08	0.11	0.13	m/s
B: Reinforcement content	0	2	4	Vol.%
C: Normal load	25	30	35	N
D: sliding distance	141	188	235	m

Table 2 L_{27} Orthogonal array design with output and S/N ratio

Run	Sliding velocity	Reinforcement content	Normal load	Sliding distance	Sp. wear rate	S/N ratio
1	0.08	0	25	141	1.5	-3.52183
2	0.08	0	30	188	1.4	-2.92256
3	0.08	0	35	235	1.4	-2.92256
4	0.08	2	25	188	1.1	-0.82785
5	0.08	2	30	235	0.97	0.26457
6	0.08	2	35	141	0.91	0.81917
7	0.08	4	25	235	1	0.00000
8	0.08	4	30	141	0.94	0.53744
9	0.08	4	35	188	0.89	1.01220
10	0.11	0	25	188	1.4	-2.92256
11	0.11	0	30	235	1.2	-1.58362
12	0.11	0	35	141	1.08	-0.66848
13	0.11	2	25	235	0.9	0.91515
14	0.11	2	30	141	0.85	1.41162
15	0.11	2	35	188	0.83	1.61844
16	0.11	4	25	141	0.91	0.81917
17	0.11	4	30	188	0.76	2.38373
18	0.11	4	35	235	0.86	1.31003
19	0.13	0	25	235	1.4	-2.92256
20	0.13	0	30	141	1.03	-0.25674
21	0.13	0	35	188	0.95	0.44553
22	0.13	2	25	141	0.81	1.83030
23	0.13	2	30	188	0.75	2.49877
24	0.13	2	35	235	0.81	1.83030
25	0.13	4	25	188	0.8	1.93820
26	0.13	4	30	235	0.68	3.34982
27	0.13	4	35	141	0.86	1.31003

S/N ratio for the determination of the relative contribution of different controlling parameters.

3. Results and Discussion

3.1 Microstructural Analysis

SEM micrograph of as-received steel and energy dispersive spectroscopic mapping of the elements are depicted in Fig. 1. As mentioned in our earlier article (Ref 28), the presence of a small amount of porosity can be observed from Fig. 1, which indicates incomplete densification. The microstructure of composite with 4 vol.% TiB_2 (Fig. 2) shows uniform distribution of TiB_2 particles, distinguished as black regions in the matrix. This observation may be due to the low temperature employed during the hot consolidation process. The existence of Ti and B elements are clearly observed in the corresponding EDX mapping of the composite. EDX mapping also revealed that TiB_2 particles are distributed mostly along the grain boundary. The detailed microstructure analysis is reported elsewhere (Ref 28, 37).

3.2 Wear Analysis

Figure 3 shows the variation of the sample's depth of wear with test duration under a constant load of 25 N and sliding speed of 0.13 m/s. This image revealed the improvement of wear performance of the composite, which can be realized from the decrease in depth of wear by incorporation of TiB_2 . Uniform distribution of reinforcement particles in the matrix and good interfacial bonding plays a significant role in such

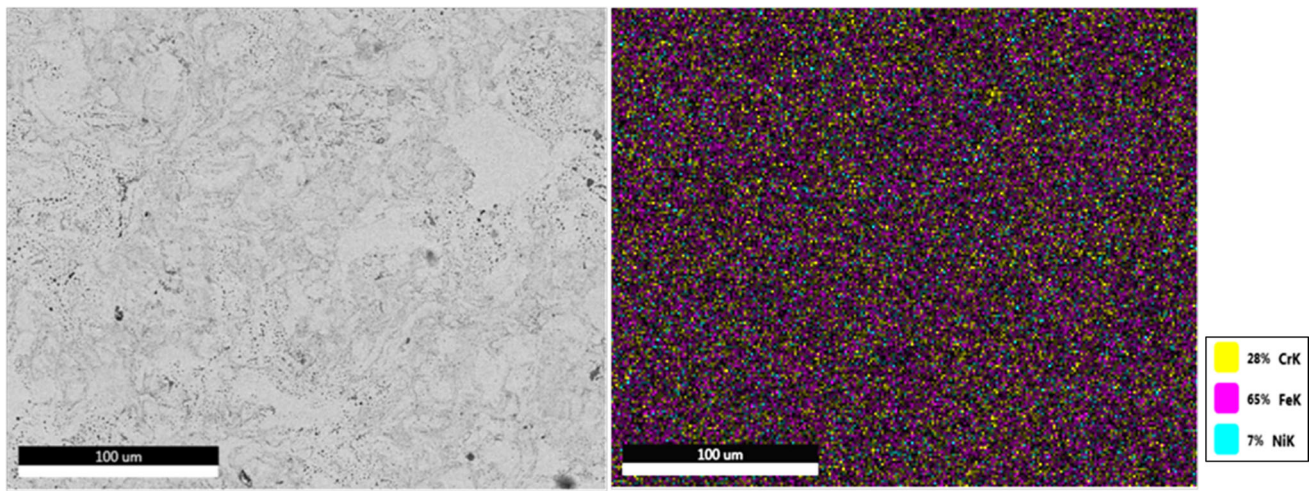


Fig. 1 Scanning electron micrograph of unreinforced steel matrix along with EDX elemental mapping

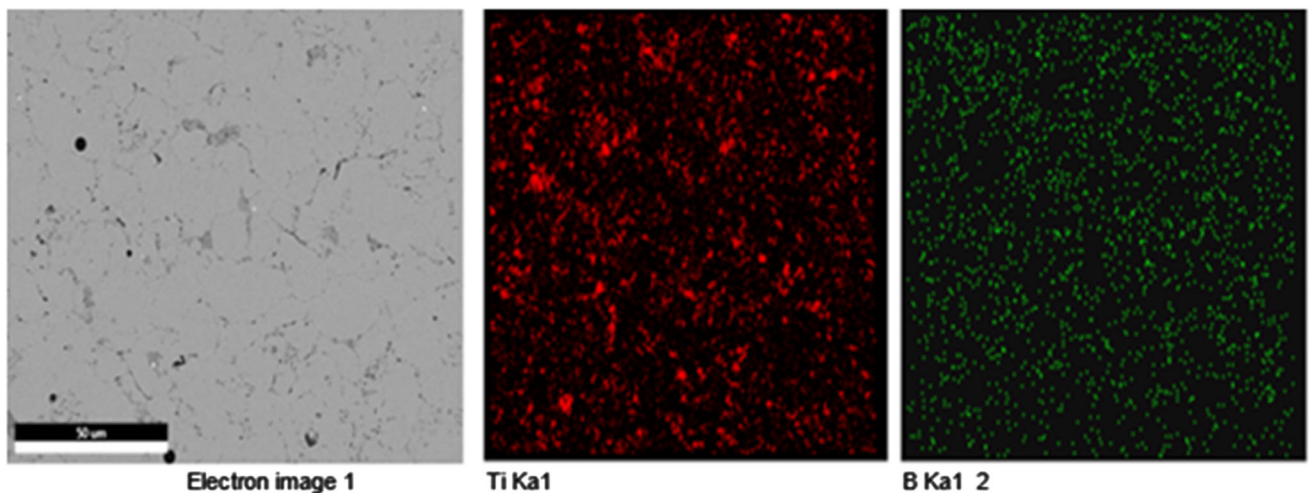


Fig. 2 Scanning electron micrograph of composites with 4 vol.% TiB_2 along with EDX elemental mapping

enhancement due to their load-bearing capacity and reduced actual contact area during wear. It is well known that sliding wear of material is a linear function of hardness (Ref 14). Because of the increasing hardness of composites with an increase in reinforcement content, the depth of wear decreases indicating better wear resistance. A reduction in wear depth could be ascribed to the reduction in the contact area between the pin and disc due to increased reinforcement particles on the sample's surface. It is worth noting that the as-received steel showed a sharp increase in “depth of wear” with test duration, whereas composites showed almost constant “depth of wear” after 500 s. It is well known that the presence of TiB_2 helps to retain strength and hardness for a longer duration, as reported in earlier studies (Ref 13, 15, 16). The wear of composite is observed to be nonlinear, as evident from Fig. 3(a). The nonlinear behavior is due to the occurrence of complex wear mechanisms of composites during sliding. Therefore, it is essential to establish the wear mechanism.

Figure 3(b) and (c) depict the depth of wear of as-received steel with test duration under a varying range of applied load and sliding speed, respectively. This image revealed an increase

in depth of wear with load at constant sliding speed. Similar results have also been obtained in the cases with varying sliding speeds under constant load, as presented in Fig. 3(c).

Figure 3(d) and (e) show the variation in depth of wear of composite with 2 vol.% TiB_2 at different loads and sliding speed. It can be seen from Fig. 3(d) that there is a slight increase in depth of wear with applied load from 25 N to 35 N. When the composite was subjected to an applied load of 25 N, the depth of wear was relatively constant after a specific testing duration. In contrast, it gradually increased with time as the load increased. This observation is due to the dominating behavior of TiB_2 particles in reducing the depth of wear at low load (25 N) and, consequently, the evolution of little damage during the test time. As the load increases, a sudden increase in depth is observed, followed by heavy noise indicating the wear mechanism's transition. Further, the variation of wear depth with sliding speed could easily be explained from Fig. 3(e), which could be attributed to an increase in temperature at the interface due to an increase in sliding speed over the counter face material. It is also evident from Fig. 3(e) that the depth of wear is relatively small when the sliding speed is low, and it

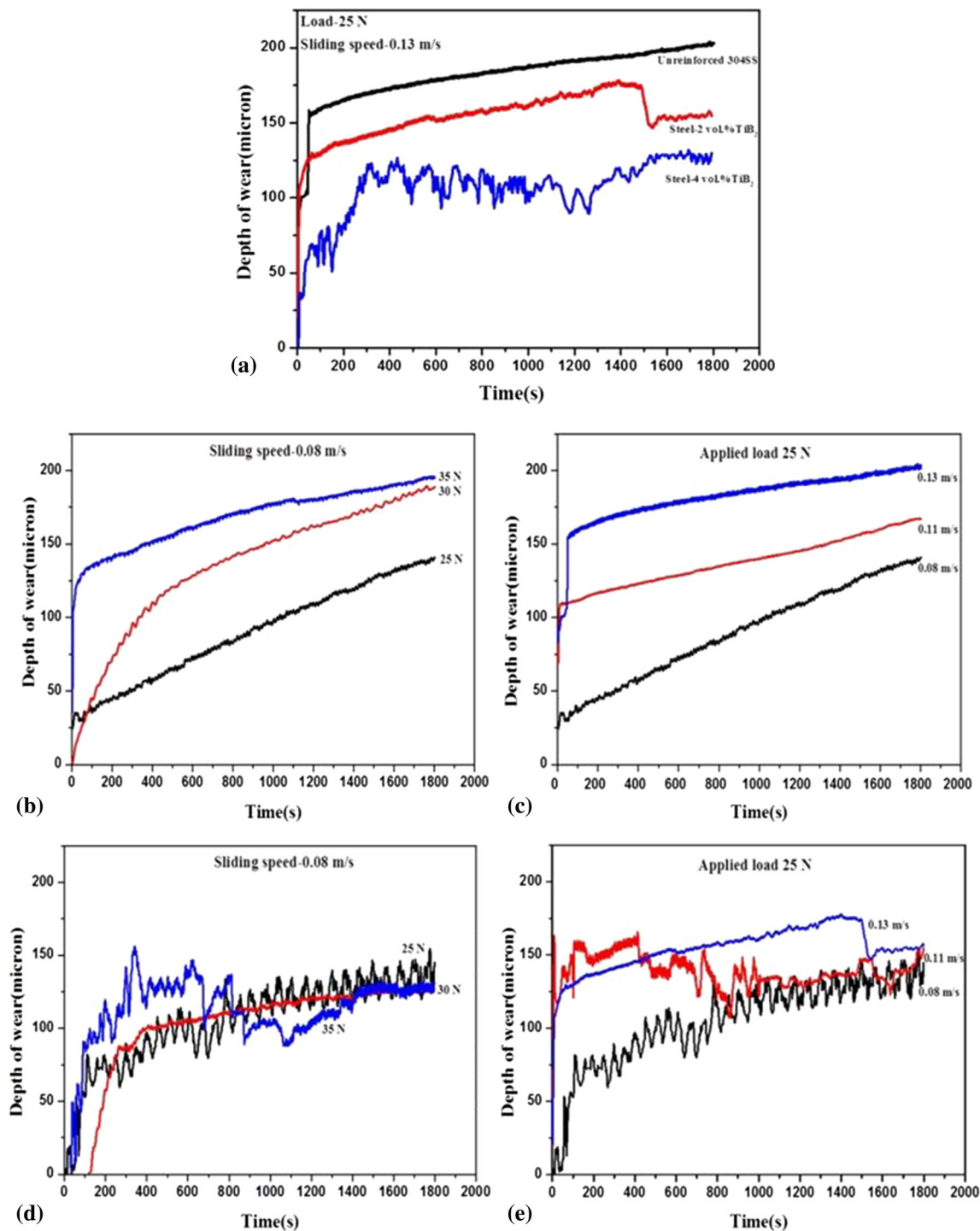


Fig. 3 Variation in depth of wear of unreinforced and reinforced steel with test duration at different load and sliding speed

further increases with an increase in sliding speed. Of all the samples, as-received steel exhibited the highest wear depth at all sliding speeds and applied loads compared to that of composites, which is in line with Archard's wear law.

Figure 4 presents the variation of volume loss of as-received steel and the composites. The volume loss of as-received steel is about 26 and 33% higher than the composite with 2 and 4 vol.% TiB₂, respectively. The presence of hard TiB₂ particles increased the hardness and load-bearing ability of the composites. Again, enhancement in wear performance of composite

containing 4 vol.% TiB₂ can be observed as compared to 2 vol.% TiB₂ reinforced composite. The decrease in volume loss in composites confirms uniform distribution of particles during hot pressing employed in the present work. Many authors have stated high wear resistance of composites with hard reinforced particles due to reduced actual contact between the matrix and counterpart (Ref 38-40). Generally, the presence of fine and well-dispersed particles in the matrix influences the wear rate and provides a localized area of high-stress concentration. Additionally, an increase in reinforcement content improves the

wear performance by reducing particle mean free path and restricting the matrix's deformation.

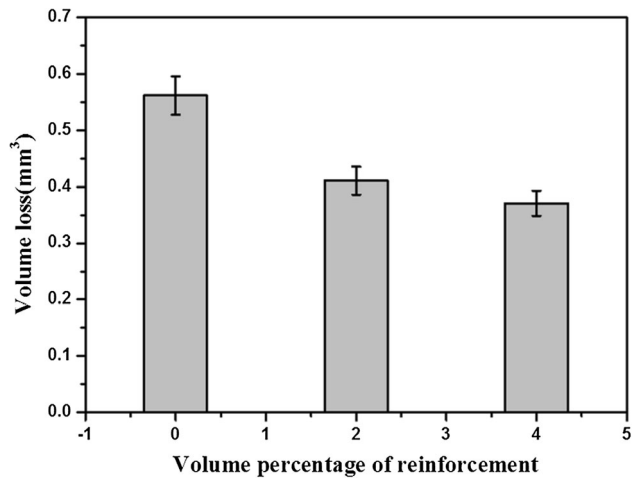


Fig. 4 Variation of volume loss of investigated samples with reinforcement content

Table 3 Response Table for Signal to Noise Ratios under Smaller is better characteristics

Level	A	B	C	D
1	-0.84016	-1.91949	-0.52133	0.25341
2	0.36483	1.15116	0.63145	0.35821
3	1.11374	1.40674	0.52830	0.02679
Delta	1.95390	3.32622	1.15278	0.33142
Rank	2	1	3	4

3.3 Wear Analysis using Taguchi Experimental Design

The experimental outcomes of the specific wear rate of composites and the corresponding S/N ratio according to L_{27} orthogonal design are presented in Table 2. The average of three experimental values of the wear rate is taken as the final value for each run. The last column of the table shows the calculated values of the S/N ratio for each test run. All the analysis was done by using MINITAB 14 software. Table 3 presents the S/N ratio response under “smaller-is-better” characteristics. The control factor’s significance can be observed from the assigned rank, as shown in the Table 3.

In this study, TiB_2 content is associated with a higher delta value, indicating the most significant factor. Figure 5 shows the main effect plot for S/N ratios of individual control factors. It was concluded from the graphical analysis that minimum wear could be obtained with the combination of A_3 , B_3 , C_2 , and D_2 . Under this set of process parameters, wear trials have been conducted and found to be minimum, i.e., 0.68. The response surface analysis was also carried out to compare the model results (Table 4).

3.4 Statistical Analysis

The analysis of obtained test results using Taguchi’s L_{27} orthogonal array resulted that reinforcement content followed by sliding velocity and normal load have the highest significant impact on the wear rate. Hence, in order to study the effect of the significant control factors more precisely on the wear rate, test trials are conducted considering a wide range of the individual significant test parameters within the experimental domain by keeping all the other parameter levels constant. The outcomes of the test trials are depicted in Figs. 6, 7 and 8, respectively. The test trials are conducted considering a sliding distance of 141m.

Figure 6 illustrates the variation in specific wear rate with reinforcement content at three different sliding velocities (0.08 m/s, 0.11 m/s and 0.13 m/s) and Fig. 6(a), (b) and (c) are the plots showing this relation at normal loads of 25 N, 30 N and 35 N, respectively. From the figures, it is clearly evident that

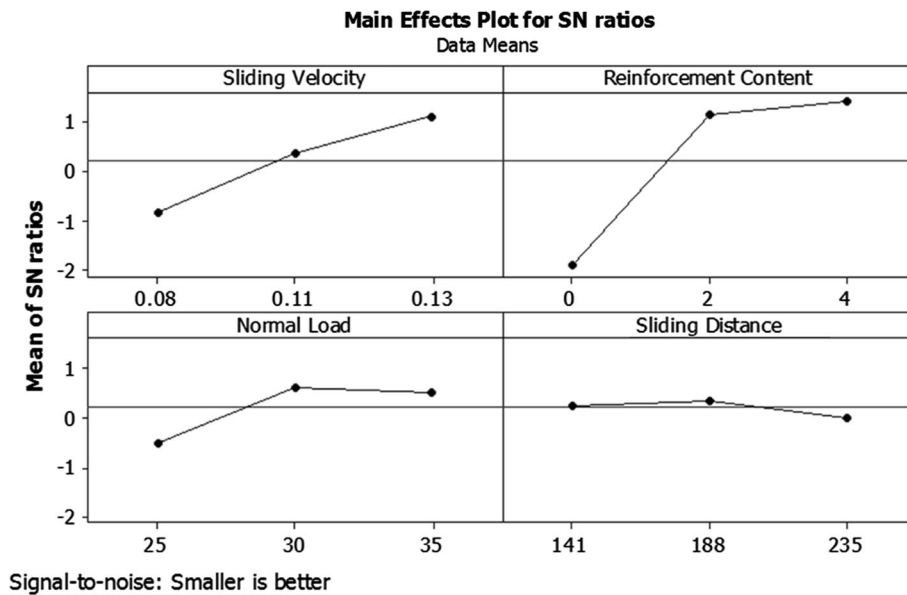


Fig. 5 Main effect plot for S/N ratio of individual control factors

Table 4 ANOVA Table for specific wear rate

Control factors	DOF	SS	Variance	F test	<i>p</i>	Percentage of contribution
Sliding velocity	2	0.23381	0.00044	16.32	0.0	16.5
reinforcement content	2	0.93383	2.769	65.17	0.0	65.86
Normal load	2	0.11299	17.208	7.89	0.003	7.97
Sliding Distance	2	0.00832	1529.31	0.58	0.570	0.6
Error	18	0.12896				9.1
Total	26	1.41790				100

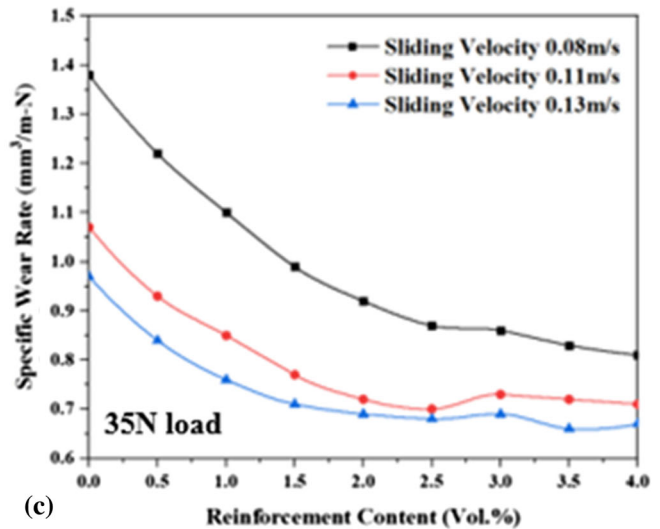
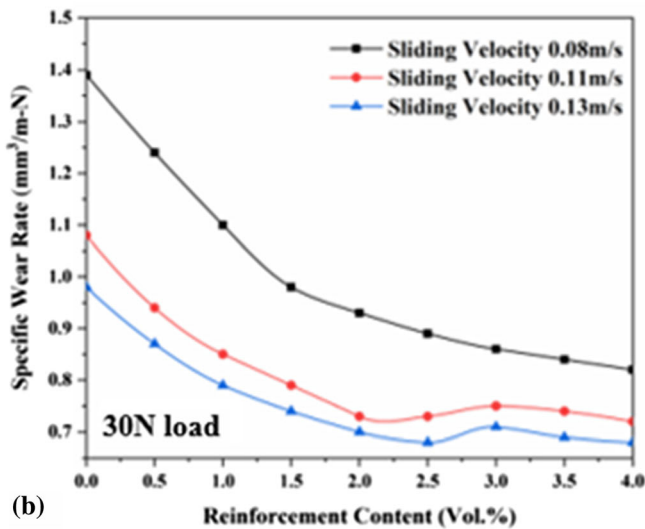
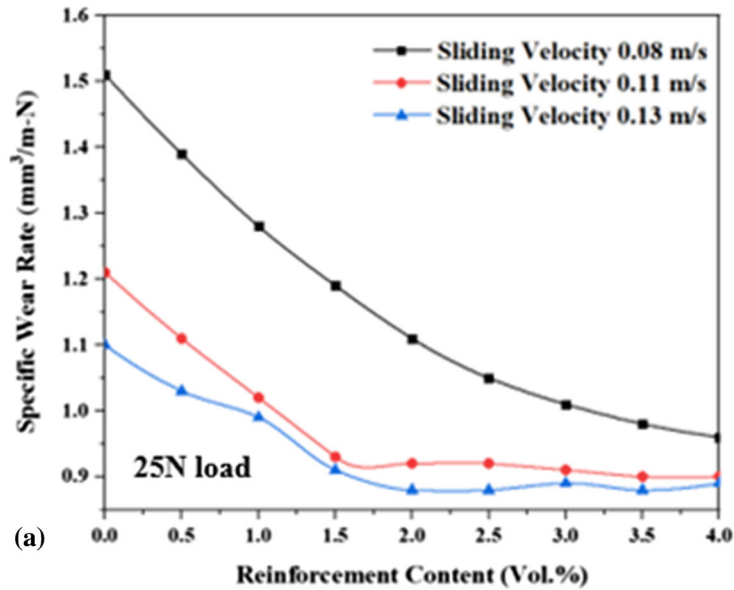


Fig. 6 Specific wear rate with reinforcement content at different sliding velocities

the wear rate is decreased with the increase in reinforcement content. At low sliding velocity (0.08 m/s) the curve presenting the wear rate is apparent to be flat after a reinforcement content of 3 vol.% indicating the appearance of steady state wear loss beyond which the reinforcement content will not affect the wear rate more significantly. Whereas, for higher sliding velocity, the steady state is attained at the reinforcement content of 2 vol.%. Identical observations have been reported by Akhtar and Guo

(Ref 11), Pagounis and Lindross (Ref 12), sulima (Ref 13), and Tjong and Lau (Ref 14) in their respective investigations.

The variation in specific wear rate of the unreinforced and reinforced composites corresponding to the normal load at three different sliding velocities (0.08 m/s, 0.11 m/s and 0.13 m/s) are displayed in Fig. 7(a), (b) and (c), respectively. The wear rate of both the unreinforced and reinforced composites as witnessed from the figures is decreased with the increase in normal load up to a certain extent and beyond that no significant variation in

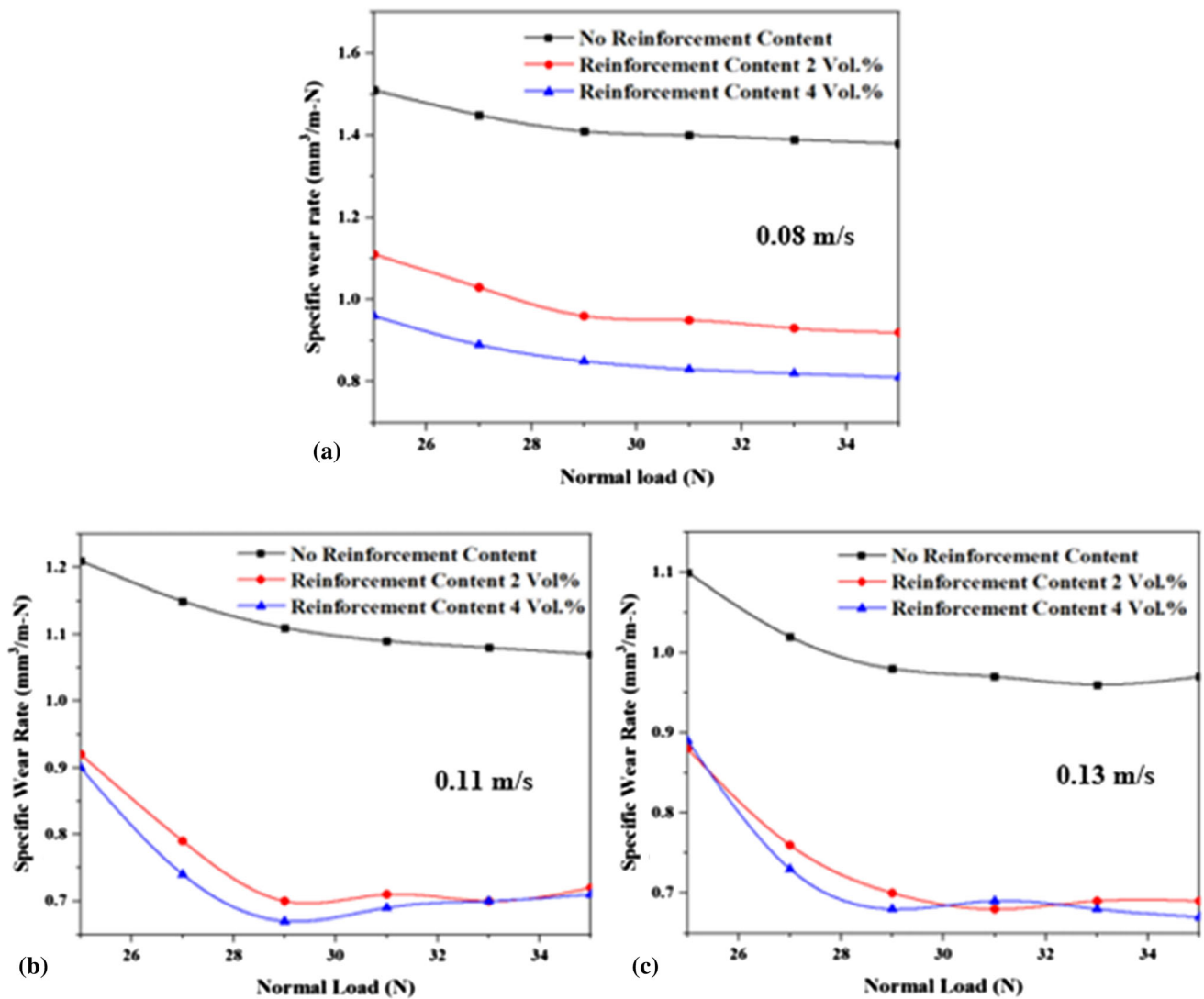


Fig. 7 Specific wear rate of the reinforced and unreinforced composites with normal load at different sliding velocities

the wear rate is observed with the increase in normal load. The figures confirmed that for both the unreinforced and reinforced composites, the steady state is attained beyond a normal load of 29N. Bastwros et al. (Ref 41) reported similar observation of increased material ploughing at higher load. They also suggested excessive subsurface damaging and delamination with the increase in applied load. These findings follow Archard's equation of wear that states the wear is low at a lower value of applied loads and increases with a constant ratio (Ref 42). An increase in the applied load results in a rise in the localized temperature at the interface that leads to deformed surface layers and adhesion, and consequently, an increase in wear rate. It can be noticed from Fig. 10 that the specific wear rate of as-received steel decreased sharply with load compared to that of composites. However, there is a slight change in the wear rate of composites at higher loads. This result confirms the presence of TiB₂ is beneficial in improving the wear resistance of steel composites.

Similarly, Fig. 8 displays the wear rate of the composites consisting of 0, 2 and 4 vol.% of reinforcement contents corresponding to the sliding velocity. Fig. 8(a), (b) and (c) are the representatives of the variation plots at three different

normal loads (25 N, 30 N and 35N), respectively. The specific wear rate was found to be decreased with the increase in sliding velocity. However, it is witnessed that the wear rate of the as-received steel is much higher than the reinforced ones. This decrease in specific wear rate with the increase in speed can be related to the rise in surface temperature (Ref 43, 44). Hence, additional severe wear due to adhesion and deformation was informed by the researchers in earlier investigation (Ref 45-47). At higher sliding speed, the composite has higher volume loss indicating easy removal of reinforcement particles at a higher speed. Commonly, composite's wear resistance is improved by the presence of hard particles due to their load-bearing ability and the reduced contact area between the composite and counterpart disc. At a higher speed, the bonding effect of the reinforced particles and the matrix usually reduces due to the matrix material's microthermal softening.

3.5 Analysis of Worn Surfaces

Detail analysis of the worn-out surfaces by a field emission scanning electron microscope (Supra 55, Zeiss, Germany) was performed to study the wear mechanism involved in the material. The SEM images of the worn surface of the observed

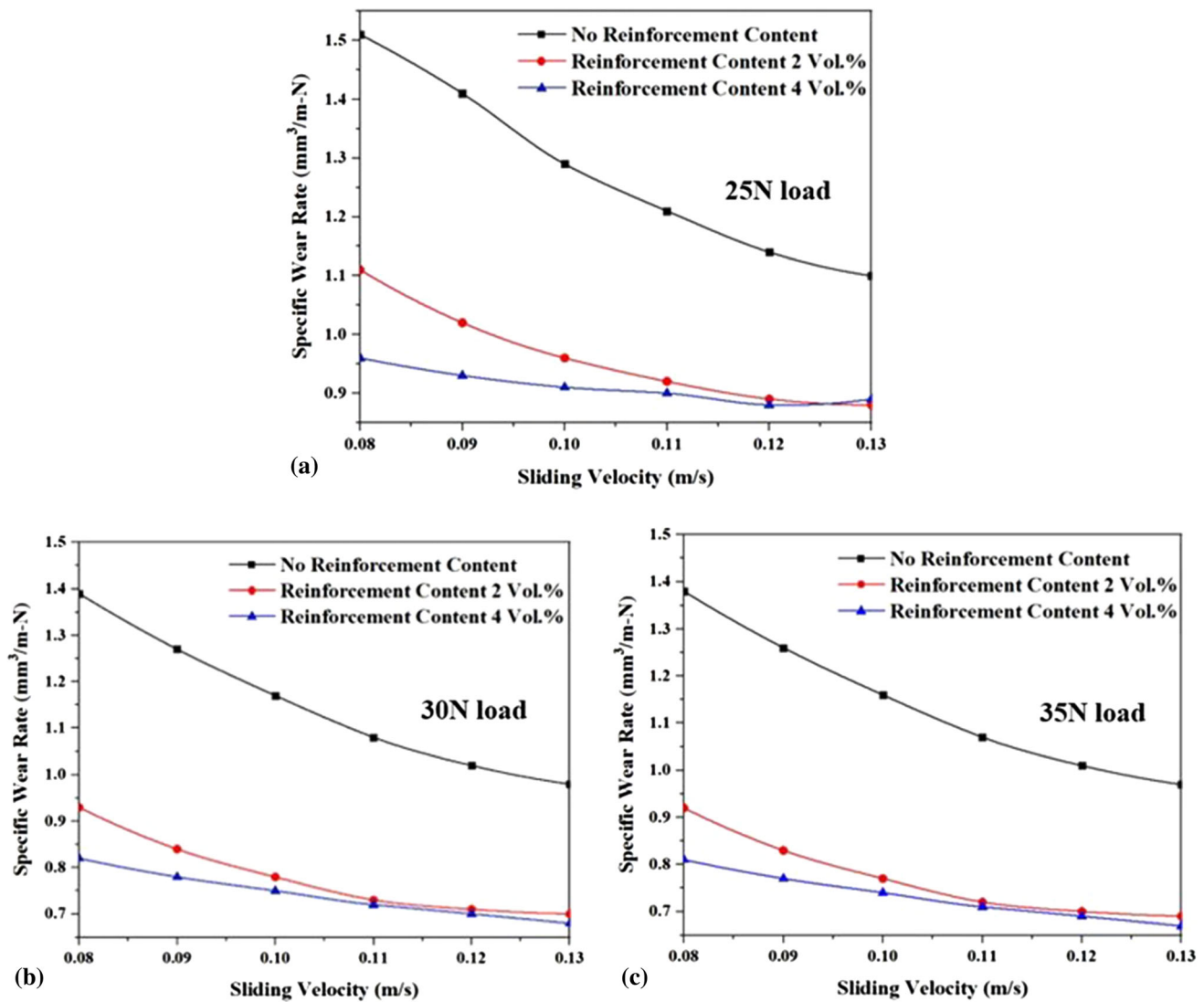


Fig. 8 Specific wear rate of the composites as a function of sliding velocity

samples under the load of 25 N and sliding speed 0.08 m/s are shown in Fig. 9. The sliding directions are indicated by arrow marks in the micrographs. Adhesive wear mechanism is found to be the dominant mechanism in as-received steel due to observation of deformation in the form of grooving, delamination, and micro ploughing. The worn surface has undergone significant plastic deformation along the sliding direction. The surface of as-received steel as shown in Fig. 9(a) reveals a high amount of wear in an irregular manner over a huge area. The surface is severely damaged with the formation of deep grooves and pit which is the property of the adhesive wear mechanism. The hardness of as-received steel (380 HV-423 HV) is lower than that of steel reinforced with TiB₂ particles (570 HV-675 HV) (Ref 48) and consequently, the wear resistance, which is consistent with the findings that lower the hardness, higher is the wear (Ref 47).

However, analysis of the worn surface of TiB₂ reinforced steel reveals improved wear performance by inhibiting plastic ploughing and cutting. It can be inferred the worn surface has hardly undergone plastic deformation due to the presence of TiB₂ particles indicating strong resistance to plastic deformation and wear (Fig. 9b, c). The addition of TiB₂ to the as-

received steel results in the formation of continuous grooves parallel to sliding direction on the worn surface. This may be ascribed to the distribution of hard TiB₂ particles in the matrix and reduction in the wear contact area. The variation in the worn surface characteristics is closely related to the transition of wear mechanism in the reinforced steel during the sliding wear process. It is obvious that the wear mechanism is changed from adhesive wear to abrasive wear owing to the absence of flake-like wear scars on the surface (Ref 49).

Further, the abrasion grooves become smoother and closely spaced with increase in TiB₂ content, signifying enhanced wear resistance (Fig. 9c). Increase in TiB₂ content from 2 to 4 vol.% prevents the surface damage by reducing severe plastic deformation of the surface as shown in Fig. 9(c). In general, the wear performance of composite materials improves with an increase in reinforcement content owing to enhanced hardness and sliding action of a large number of hard particles. Henceforth, larger TiB₂ content in the composite enhanced the wear resistance by reducing contact area and delaying the material removal during sliding. In addition, it is well known that shallow and parallel grooves pattern represent abrasive wear mechanisms during sliding wear of composites. Based on

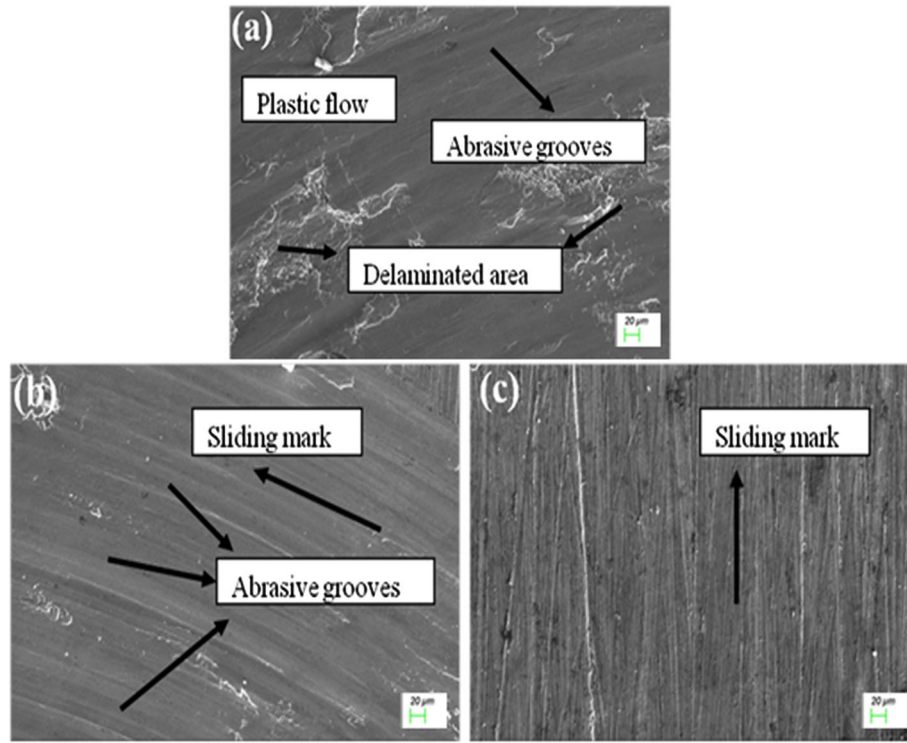


Fig. 9 SEM images of worn surfaces of (a) unreinforced steel, (b) steel matrix composite with 2 vol.% TiB₂, (c) steel matrix composite with 4 vol.% TiB₂ under the load of 25 N and sliding speed 0.08 m/s

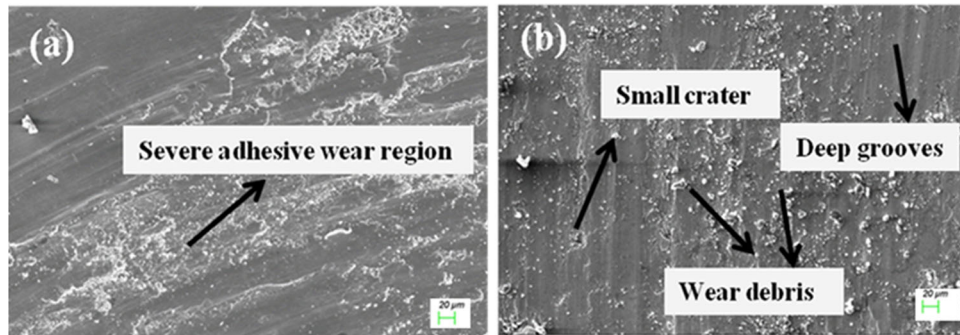


Fig. 10 SEM images of worn surfaces of (a) unreinforced steel, (b) steel matrix composite with 2 vol.% TiB₂ under the load of 35 N and sliding speed 0.08 m/s

the above wear surface characteristics, it can be concluded that the main wear mechanism is the abrasive wear mechanism in this sample. The addition of hard TiB₂ particles substantially enhances the bonding strength, softening temperature of the matrix and this greatly minimizes the wear loss as contrasted to as-received steel.

SEM images of worn surface of as-received steel and reinforced composite under the load of 35 N and sliding speed of 0.08 m/s are presented in Fig. 10(a) and (b). It is obvious from the micrographs that the amount of plastic deformation is very high on the surface of the as-received steel showing a severe adhesive wear mechanism. The worn surface of composites also revealed breaking and falling off particles which is detrimental to the wear performance. Further, the composite samples also revealed the presence of small craters

along with deep grooves generated due to the sliding action of hard counter surface pin (high chromium 100Cr₆ ball with hardness of 62HRC) on the composite surface causing ploughing on the surface which indicates adhesive wear is also operative at higher load along with abrasive wear. The extent of worn surface deterioration and groove size increases with an increase in applied load in both as-received steel and the composite. This observed wear mechanism could be confirmed from severe surface damage, a large amount of plastic flow, presence of wear debris, and delamination with an increase in load as presented in Fig. 10. Compared to the worn surface of reinforced steel, the wear surfaces of as-received steels are severely damaged (Fig. 10a), showing a great number of delamination, pits, cracks, wear debris. Although there was minimal adhesion in the composite as compared to as-received

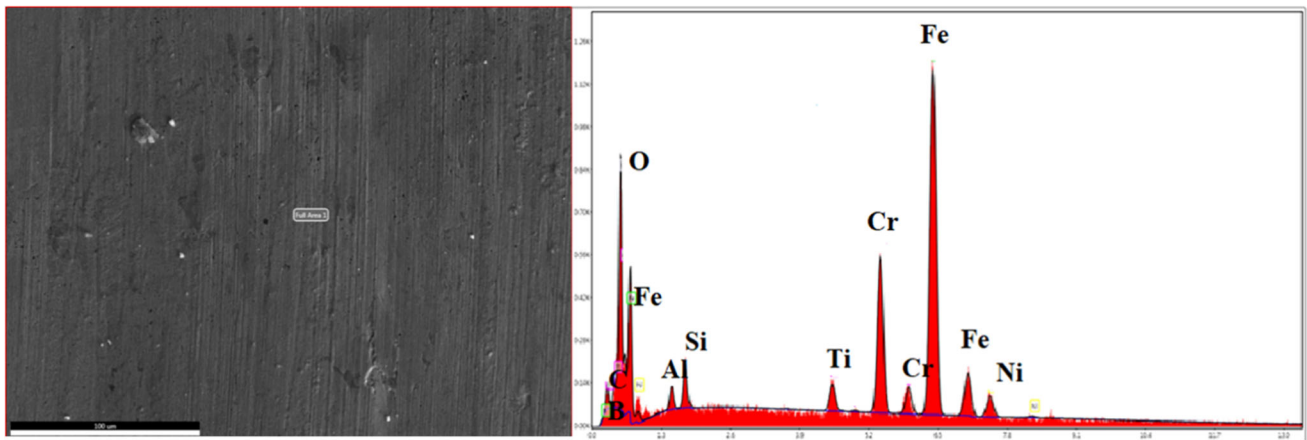


Fig. 11 SEM images of worn surfaces of composite with 4 vol.% TiB_2 under the load of 35 N and sliding speed 0.08 m/s along with EDX of the full area

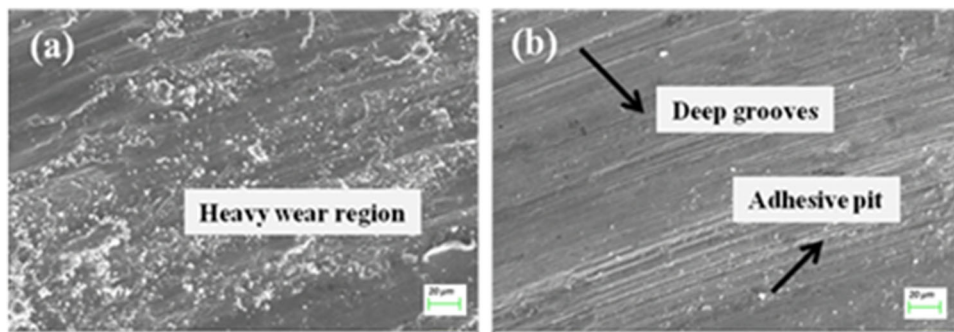


Fig. 12 SEM images of worn surfaces of (a) unreinforced steel, (b) steel matrix composite with 2 vol.% TiB_2 under the load of 25 N and sliding speed 0.13 m/s

steel, but rapid wear was observed due to increased friction under higher normal load. The outcome signifies that an increase in load exacerbates the wear due to debonding of TiB_2 particles and delamination from the matrix to become wear debris at higher load.

The worn-out surface of composite with 4 vol.% TiB_2 under the load of 35 N and sliding speed 0.08 m/s along with EDX of the full area is shown in Fig. 11. From the images it is inferred that the surface of the composites shows deeper grooves and pits due to dislodging of TiB_2 particles and their entrapment at the interface at a higher normal load, indicating an increased wear rate. Compared to the worn surfaces of composite with 2 vol.% TiB_2 , the worn surface of composite with 4 vol.% TiB_2 is less severely damaged, exhibiting a smaller number of delamination, wear debris, and deeper grooves. EDX analysis revealed the presence of Fe, Cr, Ni, Ti, B, O on the worn surface. The presence of oxygen peak confirms the existence of oxide at the selected normal load. Dispersion of reinforcement particles in the matrix act as a barrier between the mating surfaces and reduces the adhesion between the sliding surfaces. In this case, the wear rate is significantly improved without causing any surface damage. In light of the above results, it can be inferred that the hard TiB_2 particles protect the matrix efficiently during sliding owing to its load-bearing capacity and resistance to plastic deformation.

Figure 12(a) and (b) illustrate the SEM images of the worn surfaces of the as-received steel and composites with 2 vol.% TiB_2 at sliding speed of 0.13 m/s and load of 25 N. The worn surfaces of both the material were characterized by fragmentation of particles in the matrix. In addition, continuous longitudinal grooves parallel to the sliding direction are deeper with the increase in speed (Fig. 12b). The observed characteristics from the worn surface of the samples at high sliding speed indicate that abrasive and adhesive wear is the dominant wear mechanism. Hence, an increase in sliding speed is quite effective for the deterioration of wear resistance. From Fig. 12(b), it is observed that the pits mostly exist in the wear track of the composite due to the removal of reinforcement particles. As explained earlier, the dominant wear mechanism is abrasion wear in the reinforced composites. Upon increasing the sliding speed, the dominant abrasive wear mechanism is changed to mixed abrasive and adhesive wear. Analysis of the worn surface of the composite tested at sliding speed 0.13 m/s reveals the severity of wear compared to the composite at sliding speed 0.08 m/s. The higher the sliding speed, the deeper the wear grooves and the larger the wear volume. The pits may be caused by the wear surface falling off in the form of the delamination. This type of wear mechanism represents an adhesive wear mechanism. It is consistent with other researchers' observations of an increase in the number and size

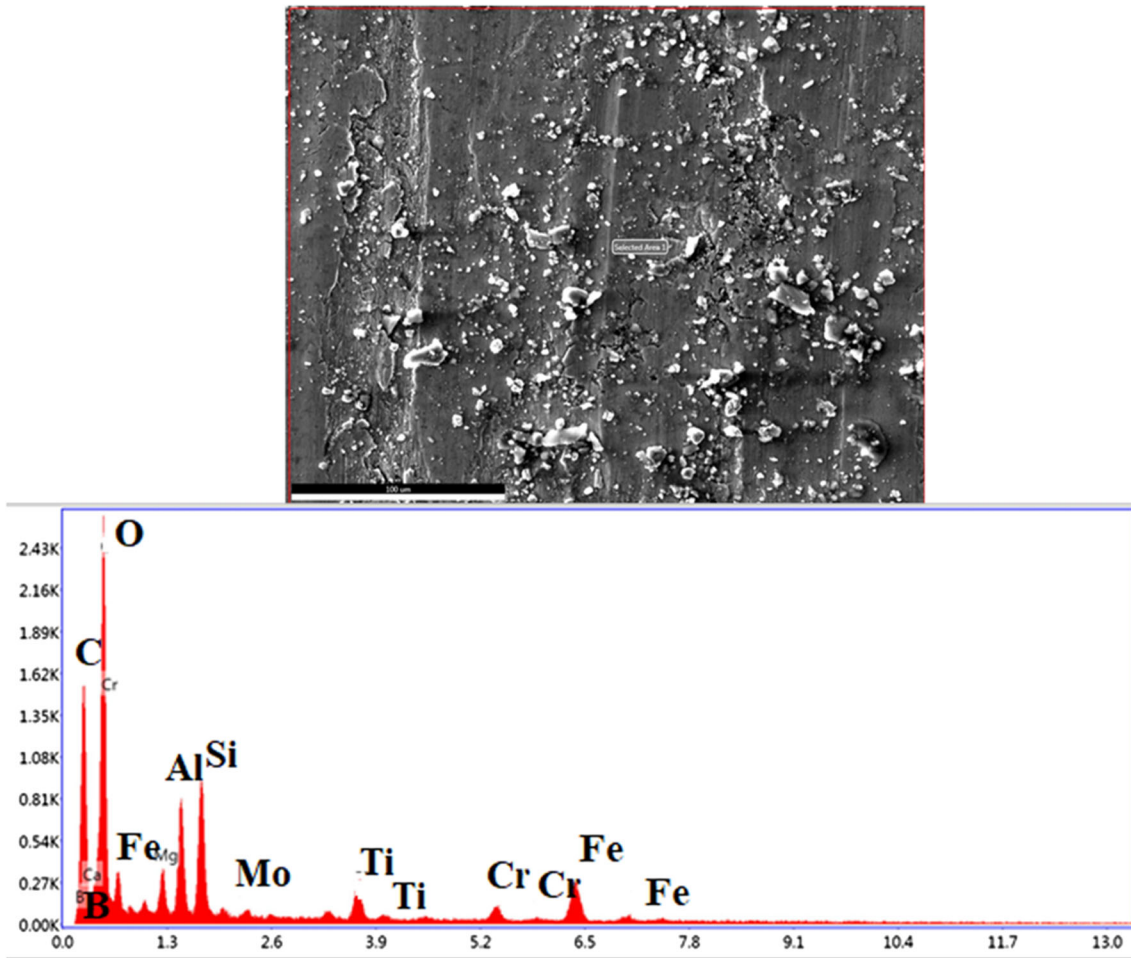


Fig. 13 EDS of worn surface morphology of 4 vol.% TiB₂ under the load of 25 N and sliding speed 0.13 m/s

of spalling pits, cracks and delamination on the wear surfaces with the increase in sliding speed.

Oxidation wear mechanism is also identified from the worn surface analysis of composite with 4 vol.% TiB₂ under the load of 25 N and sliding speed 0.13 m/s (as shown in Fig. 13). EDX analysis confirmed the presence of a high-intensity peak of oxygen, illustrating the formation of oxide on the surface. As the sliding proceeds, these oxides may be formed due to heat generated by sliding friction and the reaction of metallic debris on the worn surface. Usually, oxidation wear occurs by the generation of frictional heat during the sliding process. The presence of oxide acts as a barrier between the mating surfaces and prevents direct contact and adhesion between the sliding surfaces (Ref 50). The surface also revealed delamination and debris, produced by abrasion of the dislodged micro TiB₂ particles. It can be concluded that oxidation wear also plays a major role along with abrasive wear in the composite at the selected testing parameters. The presence of oxide and hard TiB₂ particles support reducing grooves and surface and consequently, lesser wear. However, the negative impact of higher sliding velocity and load was also revealed from the analysis of the worn surfaces of composites.

In the present work, composite with 4 vol.% TiB₂ under the load 30 N and sliding velocity 0.13 m/s reveals minimum wear under selected testing parameters as per Taguchi results. Analysis of the worn surface of this sample is performed and

shown in Fig. 14. From the image, it is inferred that the surface shows a cleaner surface with shallow parallel grooves without any crack or debris. The wear mechanism is mostly abrasive with distinct parallel grooves without any indication of plastic deformation on the worn surface. This observation indicates improved wear resistance without causing any surface distortions under the selected testing condition. Fig. 14 also presents the elemental mapping of the composite which confirms the presence of TiB₂ along with their distribution in the matrix. The presence of these hard particles on the worn surface indicates enhanced resistance to wear owing to their resistance to crack formation and reduced abrasion. The reduction in wear of this optimum sample can be accredited to compaction of wear debris containing specimen material under the selected testing parameters that protect the specimen from further wear.

4. Conclusions

The experimental investigation on the sliding wear behavior of TiB₂ reinforced hot-pressed steel composites leads to the following important conclusions.

1. The composites containing TiB₂ particles exhibited an improvement in wear performance as compared to the unreinforced part. This observation could be related to

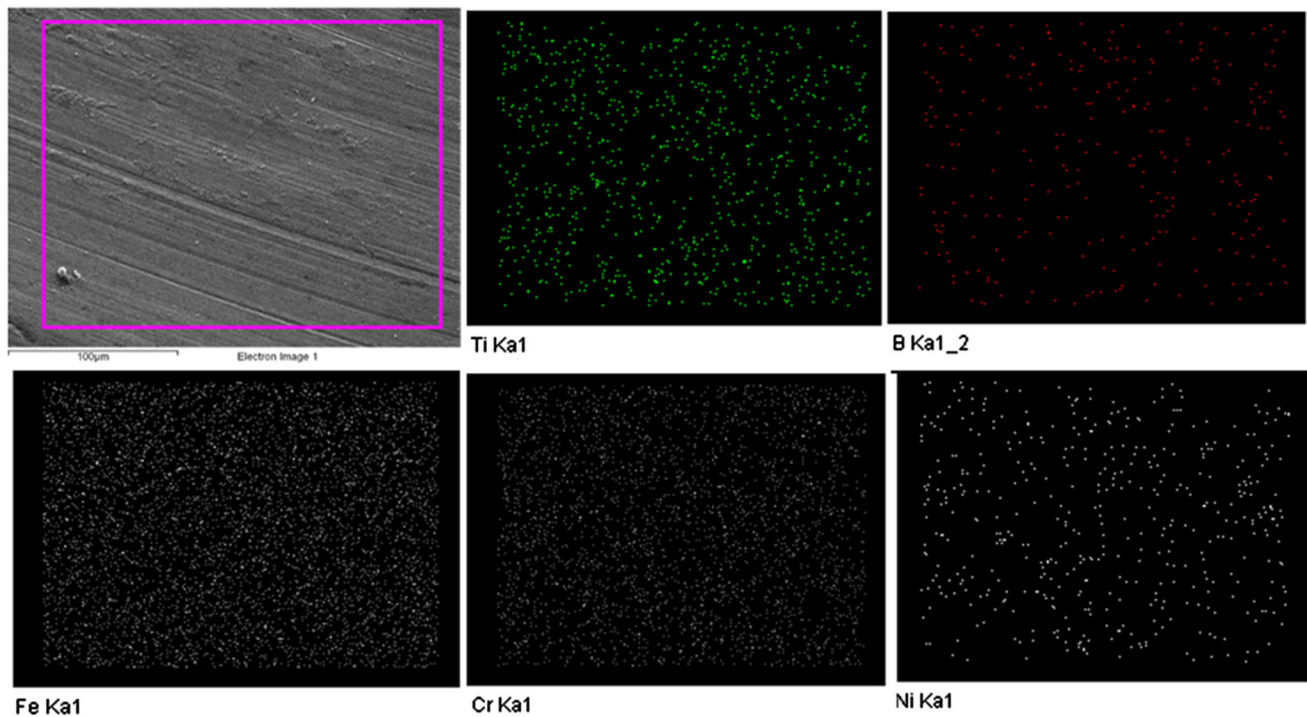


Fig. 14 SEM image of composite with 4 vol.% TiB₂ under the load 30 N and sliding velocity 0.13m/s along with elemental mapping

the high hardness of TiB₂ that hinders the direct contact between matrix and counterpart during sliding. The resultant composite's specific wear rate is in the range of 0.68-1.4 mm³/m.N depending upon the TiB₂ content.

- The specific wear rate results revealed a slightly decreasing trend with increased applied load and sliding speed under the present sliding conditions. On the contrary, as-received steel resulted in a linear decrease in the specific wear rate with the increased applied load.
- From the Taguchi experimental design, reinforcement content was the most significant factor influencing composite's wear rate, followed by sliding velocity and normal load. ANOVA is validating the same. Three-dimensional surface plots revealed reinforcement content as the most significant parameter having a higher slope than other factors.
- The composite's worn surface analysis illustrated a smoother surface than the as-received steel, characterized by deep grooves and plastic deformation. The predominant wear mechanism was a mixture of adhesive, delamination, and abrasive wear at higher load and sliding speed. Although the addition of TiB₂ improved composite's wear performance, it could not improve the wear behavior at the severe sliding condition.

Overall, the wear performance of the developed composites improved significantly at all test conditions compared to that of as-received steel due to the presence of TiB₂ as the load-bearing constituent. With improved mechanical and tribological properties, these composites can be proposed to be used for advanced engineering applications including wear and corrosion resistant parts in chemical and process industries, transportation and chemical industries, development of wear resistant parts in mining and earth moving operation and metal

forming tool for extrusion dies and rolling mills, cutting tool, forming tools etc.

Acknowledgment

The authors are grateful to the Director, CSIR-IMMT, Bhubaneswar for supporting and allowing to publish this research work.

Funding
This work was supported by the Board of Research in Nuclear Science (BRNS) of the Department of Atomic Energy (DAE), Government of India under grant no. 36(2)/14/18/2016- BRNS.

References

- G. Mahajan, N. Karve, U. Patil, P. Kuppan and K. Venkatesan, Analysis of Microstructure, Hardness and Wear of Al-SiC-TiB₂ Hybrid Metal Matrix Composite, *Indian J. Sci. Technol.*, 2015, **8**(January), p 1-6.
- V. Umasankar, Experimental Evaluation of the Influence of Processing Parameters on the Mechanical Properties of SiC Particle Reinforced AA6061 Aluminium Alloy Matrix Composite by Powder Processing, *J. Alloys Compd.*, 2014, **582**, p 380-386.
- S.Z. Abbas, Fe - TiB₂ Composites Produced through Casting Technique, *Mater. Sci. Technol.*, 2020, **36**(3), p 299-306.
- W. Gao, Y. Zhou, X. Han, S. Li and Z. Huang, Preparation and Microstructure of 3D Framework TiC - TiB₂ Ceramics and Their Reinforced Steel Matrix Composites, *Ceram. Int.*, 2021, **47**(2), p 2329-2337. <https://doi.org/10.1016/j.ceramint.2020.09.075>
- M. Sadhasivam, S.R. Sankaranarayanan and S.P.K. Babu, ScienceDirect Synthesis and Characterization of TiB₂ Reinforced AISI 420 Stainless Steel Composite through Vacuum Induction Melting Technique, *Mater. Today Proc.*, 2020, **22**, p 2550-2558. <https://doi.org/10.1016/j.matpr.2020.03.385>
- F. Qiu, H. Zhang, C.L. Li, Z.F. Wang, F. Chang, H.Y. Yang, C. De Li, X. Han and Q.C. Jiang, Simultaneously Enhanced Strength and Toughness of Cast Medium Carbon Steels Matrix Composites by Trace

- Nano-Sized TiC Particles, *Mater. Sci. Eng. A*, 2021, **819**, p 141485. <https://doi.org/10.1016/j.msea.2021.141485>
7. B. Almgour, D. Grzesiak and J.M. Yang, Rapid Fabrication of Bulk-Form TiB₂/316L Stainless Steel Nanocomposites with Novel Reinforcement Architecture and Improved Performance by Selective Laser Melting, *J. Alloys Compd.*, 2016, **680**, p 480–493.
 8. I. Sulima, P. Putyra, P. Hyjek and T. Tokarski, Effect of SPS Parameters on Densification and Properties of Steel Matrix Composites, *Adv. Powder Technol.*, 2015, **26**(4), p 1152–1161.
 9. I. Sulima, P. Klimczyk and P. Malczewski, Effect of TiB₂ particles on the Tribological Properties of Stainless Steel Matrix Composites, *Acta Metall. Sin. English Lett.*, 2014, **27**(1), p 12–18.
 10. A. Farid, S. Guo, X. Yang and Y. Lian, Stainless Steel Binder for the Development of Novel TiC-Reinforced Steel Cermets, *J. Univ. Sci. Technol. Beijing Miner. Metall. Mater.*, 2006, **13**(6), p 546–550.
 11. F. Akhtar and S.J. Guo, Microstructure, Mechanical and Fretting Wear Properties of TiC-Stainless Steel Composites, *Mater. Charact.*, 2008, **59**(1), p 84–90.
 12. E. Pagounis and V.K. Lindroos, Processing and Properties of Particulate Reinforced Steel Matrix Composites, *Mater. Sci. Eng. A*, 1998, **246**(1–2), p 221–234.
 13. I. Sulima, Tribological Properties of Steel/TiB₂ Composites Prepared by Spark Plasma Sintering, *Arch. Metall. Mater.*, 2014, **59**(4), p 1263–1268.
 14. S.C. Tjong and K.C. Lau, Sliding Wear of Stainless Steel Matrix Composite Reinforced with TiB₂ Particles, *Mater. Lett.*, 1999, **41**(4), p 153–158.
 15. S.C. Tjong and K.C. Lau, Abrasion Resistance of Stainless-Steel Composites Reinforced with Hard TiB₂ Particles, *Compos. Sci. Technol.*, 2000, **60**(8), p 1141–1146.
 16. Y.P. Song, H. Yu, J.G. He and H.G. Wang, Elevated Temperature Sliding Wear Behavior of WCP-Reinforced Ferrous Matrix Composites, *J. Mater. Sci.*, 2008, **43**(22), p 7115–7120.
 17. C.C. Degnan, P.H. Shipway and J.V. Wood, Elevated Temperature Sliding Wear Behaviour of TiC-Reinforced Steel Matrix Composites, *Wear*, 2001, **251**(1–12), p 1444–1451.
 18. X. Deng, L. Huang, Q. Wang, T. Fu and Z. Wang, Three-Body Abrasion Wear Resistance of TiC-Reinforced Low-Alloy Abrasion-Resistant Martensitic Steel under Dry and Wet Sand Conditions, *Wear*, 2019, **2020**(452–453), p 203310. <https://doi.org/10.1016/j.wear.2020.203310>
 19. J. Singh and A. Chauhan, Overview of Wear Performance of Aluminium Matrix Composites Reinforced with Ceramic Materials under the Influence of Controllable Variables, *Ceram. Int.*, 2016, **42**(1), p 56–81. <https://doi.org/10.1016/j.ceramint.2015.08.150>
 20. T.R. Hemanth Kumar, R.P. Swamy and T.K. Chandrashekar, An Experimental Investigation on Wear Test Parameters of Metal Matrix Composites Using Taguchi Technique, *Indian J. Eng. Mater. Sci.*, 2013, **20**(4), p 329–333.
 21. P. Chatsirirungruang, Application of Genetic Algorithm and Taguchi Method in Dynamic Robust Parameter Design for Unknown Problems, *Int. J. Adv. Manuf. Technol.*, 2010, **47**(9–12), p 993–1002.
 22. N.C. Fei, N.M. Mehat and S. Kamaruddin, Practical Applications of Taguchi Method for Optimization of Processing Parameters for Plastic Injection Moulding: A Retrospective Review, *ISRN Ind. Eng.*, 2013, **2013**, p 1–11.
 23. M. Yazdani, A. Daryabari, A. Farshi and S. Talatahari, Application of Taguchi Method and Genetic Algorithm for Calibration of Soil Constitutive Models, *J. Appl. Math.*, 2013, **2013**, p 1–13.
 24. S. Dharmalingam, R. Subramanian, K. Somasundara Vinoth and B. Anandavel, Optimization of Tribological Properties in Aluminum Hybrid Metal Matrix Composites Using Gray-Taguchi Method, *J. Mater. Eng. Perform.*, 2011, **20**(8), p 1457–1466.
 25. S. Baskaran, V. Anandkrishnan and M. Duraiselvam, Investigations on Dry Sliding Wear Behavior of in Situ Casted AA7075–TiC Metal Matrix Composites by Using Taguchi Technique, *Mater. Des.*, 2014, **60**, p 184–192.
 26. B.M. Girish, B.M. Satish, S. Sarapure and A. Basawaraj, Optimization of Wear Behavior of Magnesium Alloy AZ91 Hybrid Composites Using Taguchi Experimental Design, *Metall. Mater. Trans. A Phys. Metall. Mater. Sci.*, 2016, **47**(6), p 3193–3200.
 27. S. Koksai, F. Ficici, R. Kayikci and O. Savas, Experimental Optimization of Dry Sliding Wear Behavior of in Situ AlB₂/Al Composite Based on Taguchi's Method, *Mater. Des.*, 2012, **42**, p 124–130.
 28. S. Sahoo, B.B. Jha, T.K. Sahoo and A. Mandal, Influence of Reinforcement and Processing on Steel-Based Composites: Microstructure and Mechanical Response, *Mater. Manuf. Process.*, 2018, **33**(5), p 564–571. <https://doi.org/10.1080/10426914.2017.1364865>
 29. X. Zhou, M. Wang and H. Zhao, Microstructure Characteristics of High Borated Stainless Steel Fabricated by Hot-Pressing Sintering, *J. Alloys Compd.*, 2016, **665**, p 100–106.
 30. B. Dutta and F.H. Froes, Microstructure and Mechanical Properties, *Addit. Manuf. Titan. Alloy.*, 2016, **46**(2), p 41–50.
 31. O. Olaniran, B.O. Adewuyi, J.A. Omotoyinbo, A.E. Afolabi, D. Folurunso, A. Adegbola and E. Igbafen, Development of Oxide Dispersion Strengthened 2205 Duplex Stainless Steel Composite, *Leonardo Electron. J. Pract. Technol.*, 2015, **14**(26), p 129–140.
 32. T. Madhusudhan and M. Senthil Kumar, Experimental Study on Wear Behaviour of SiC Filled Hybrid Composites Using Taguchi Method, *Int. J. Mech. Eng. Technol.*, 2017, **8**(2), p 271–277.
 33. S. Spuzic, M. Zec, K. Abhary, R. Ghomashchi and I. Reid, Fractional Design of Experiments Applied to a Wear Simulation, *Wear, Elsevier*, 1997, **212**(1), p 131–139.
 34. S.D. Bolboacă and L. Jäntschi, Design of Experiments: Useful Orthogonal Arrays for Number of Experiments from 4 to 16, *Entropy*, 2007, **9**(4), p 198–232.
 35. M. Kowalczyk, Application of Taguchi and Anova Methods in Selection of Process Parameters for Surface Roughness in Precision Turning of Titanium, *Adv. Manuf. Sci. Technol.*, 2014, **38**(2), p 21–35.
 36. N. Logothetis and A. Haigh, Characterizing and Optimizing Multi-response Processes by the Taguchi Method, *Qual. Reliab. Eng. Int.*, 1988, **4**(2), p 159–169.
 37. S. Sahoo, B.B. Jha, T.S. Mahata, J. Sharma, T.S.R.C. Murthy and A. Mandal, Impression Creep Behaviour of TiB₂ Particles Reinforced Steel Matrix Composites, *Mater. Sci. Technol. (United Kingdom)*, 2018, **34**(16), p 1965–1975. <https://doi.org/10.1080/02670836.2018.1497130>
 38. M. Akbari, M.H. Shojaeefard, P. Asadi and A. Khalkhali, Wear Performance of A356 Matrix Composites Reinforced with Different Types of Reinforcing Particles, *J. Mater. Eng. Perform.*, 2017, **26**(9), p 4297–4310.
 39. B.N. Mordiyuk, G.I. Prokopenko, Y.V. Milman, M.O. Iefimov, K.E. Grinkevych, A.V. Sameljuk and I.V. Tkachenko, Wear Assessment of Composite Surface Layers in Al–6Mg Alloy Reinforced with AlCuFe Quasicrystalline Particles: Effects of Particle Size, *Microstruct. Hardness Wear*, 2014, **319**(1–2), p 84–95.
 40. S. Poria, P. Sahoo and G. Sutradhar, Tribological Characterization of Stir-Cast Aluminium-TiB₂ Metal Matrix Composites, *Silicon, Silicon*, 2016, **8**(4), p 591–599. <https://doi.org/10.1007/s12633-016-9437-5>
 41. M.M.H. Bastwros, A.M.K. Esawi and A. Wafi, Friction and Wear Behavior of Al–CNT Composites, *Wear*, 2013, **307**(1–2), p 164–173.
 42. J.F. Archard and W. Hirst, The Wear of Metals under Unlubricated Conditions, *Proc. R. Soc. London. Ser. A. Math. Phys. Sci.*, 1956, **236**(1206), p 397–410.
 43. A.R. Goswami, S. Sardar, and S.K. Karmakar, Temperature Rise and Wear of Sliding Contact of Alloy Steels, *AIP Conf. Proc.*, 2016, **1754**
 44. P. Palanikumar, N. Gnanasekaran, K. Subrahmanya and V. Kaliveeran, Effect of Sliding Speed and Rise in Temperature at the Contact Interface on Coefficient of Friction during Full Sliding of SS304, *Mater. Today Proc.*, 2020, **2020**(27), p 1996–1999. <https://doi.org/10.1016/j.matpr.2019.09.046>
 45. H. Kaftelen, N. Ünlü, G. Göller, M. Lütfi Öveolu and H. Henein, Comparative Processing-Structure-Property Studies of Al–Cu Matrix Composites Reinforced with TiC Particulates, *Compos. Part A Appl. Sci. Manuf.*, 2011, **42**(7), p 812–824.
 46. F. Velasco, W.M. Lima, N. Antón, J. Abenójar and J.M. Torralba, Effect of Intermetallic Particles on Wear Behaviour of Stainless Steel Matrix Composites, *Tribol. Int.*, 2003, **36**(7), p 547–551.
 47. P. Ravindran, K. Manisekar, R. Narayanasamy and P. Narayanasamy, Tribological Behaviour of Powder Metallurgy-Processed Aluminium Hybrid Composites with the Addition of Graphite Solid Lubricant, *Ceram. Int.*, 2013, **39**(2), p 1169–1182.
 48. S. Sahoo, B.B. Jha, T. Mahata, J. Sharma, T.S.R.C. Murthy and A. Mandal, Mechanical and Wear Behaviour of Hot-Pressed 304 Stainless Steel Matrix Composites Containing TiB₂ Particles, *Trans. Indian*

- Inst. Met.*, 2019, **72**(5), p 1153–1165. <https://doi.org/10.1007/s12666-019-01588-1>
49. R. Gecu, H. Atapek and A. Karaaslan, Influence of Preform Preheating on Dry Sliding Wear Behavior of 304 Stainless Steel Reinforced A356 Aluminum Matrix Composite Produced by Melt Infiltration Casting, *Tribol. Int.*, 2017, **115**, p 608–618.
50. M.X. Wei, K.M. Chen, S.Q. Wang and X.H. Cui, Analysis for Wear Behaviors of Oxidative Wear, *Tribol. Lett.*, 2011, **42**(1), p 1–7.

Publisher's Note Springer Nature remains neutral with regard to jurisdictional claims in published maps and institutional affiliations.